

Supplementary material for

The Effects of Ocean Surface Waves on Global Intraseasonal Prediction: Case Studies with a Coupled CFSv2.0-WW3

Ruizi Shi¹, Fanghua Xu^{1*}, Li Liu¹, Zheng Fan¹, Hao Yu¹, Hong Li^{1,3}, Xiang Li² and Yunfei Zhang²

¹Ministry of Education Key Laboratory for Earth System Modeling, and Department of Earth System Science, Tsinghua University, Beijing 100084, China

² Key Laboratory of Marine Hazards Forecasting, National Marine Environmental Forecasting Center, Ministry of Natural Resources, Beijing, 100081, China

³ Department of Atmospheric and Oceanic Sciences and Institute of Atmospheric Sciences, Fudan University, Shanghai, 200433, China.

Correspondence to: Fanghua Xu (f xu@mail.tsinghua.edu.cn)

Contents of this file

Figures S1 to S7

Tables S1 to S4

Introduction

Figures S1 is the 53-day average 10-m wind, surface current and surface Stokes drift in Jan-Feb, 2017 and Aug-Sep, 2018 and the angles between them.

Figures S2 is the Charnock parameter C_{ch} obtained by ST4-FAN in boreal winter and summer.

Figures S3 is the 53-day regression coefficient (trend) of absolute bias in CTRL.

Figures S4 is the 53-day average latent heat flux and sensible heat flux in CTRL for Jan-Feb, 2017 and Aug-Sep, 2018.

Figures S5 is the 53-day average sensible heat flux difference between 4 sensitivity experiments and CTRL in Jan-Feb, 2017 and Aug-Sep, 2018.

Figures S6 is the 53-day average difference of momentum flux, WSP10, latent heat flux and sensible heat flux between FLUX_CURR and CTRL in Jan-Feb, 2017 and Aug-Sep, 2018.

Figures S7 is the 53-day average difference of momentum flux, WSP10, latent heat flux and sensible heat flux between FLUX_ST and CTRL in Jan-Feb, 2017 and Aug-Sep, 2018.

Tables S1 shows the 28-day global average PRD and daily runtime for SST, SWH and WSP10 in sensitive experiments with different coupling step in Jan, 2017.

Tables S2 shows the correlation coefficient, RMSE and skill score of SWH simulations versus Jason-3 observation at 00:00 on Jan 3, 2017.

Tables S3 shows the 53-day mean absolute percentage error differences for WSP10 between FLUX_CURR/FLUX_ST/ FLUX and CTRL in Jan-Feb, 2017 and Aug-Sep, 2018.

Tables S4 shows the NDBC buoy identifiers.

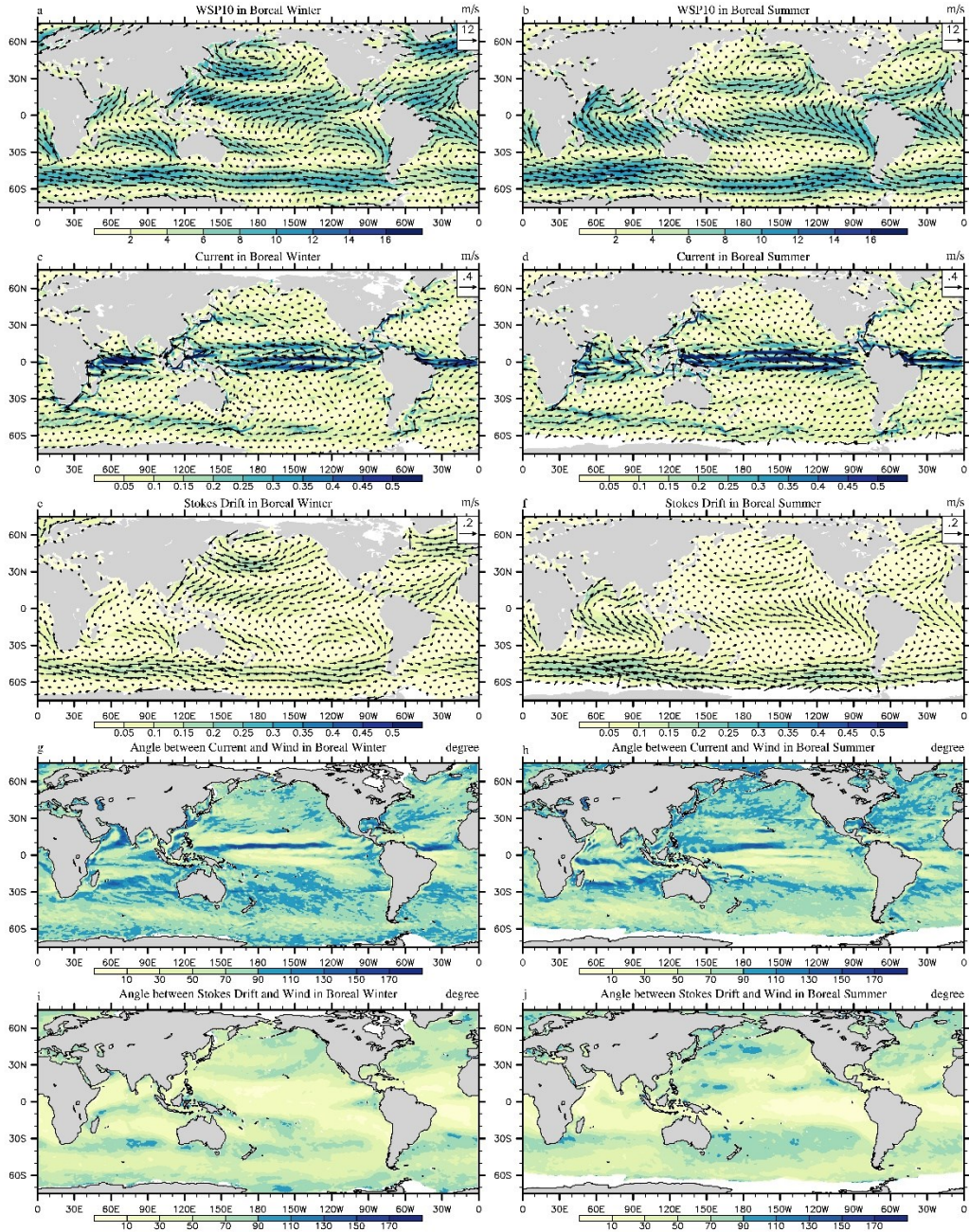


Figure S1. a, b: the 53-day average 10-m wind (m/s) in Jan-Feb, 2017 and Aug-Sep, 2018; c, d: the average ocean surface current (m/s) in Jan-Feb, 2017 and Aug-Sep, 2018; e, f: the average surface Stokes drift (m/s) in Jan-Feb, 2017 and Aug-Sep, 2018; g, h: the average angle between surface current and 10-m wind; i, j: the average angle between surface Stokes drift and 10-m wind.

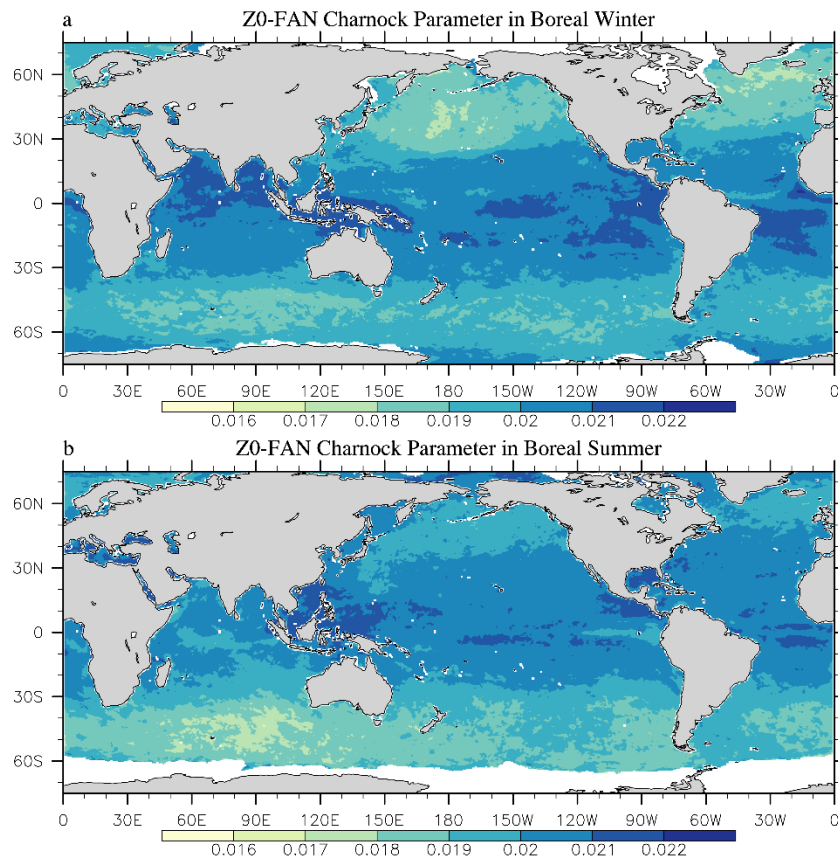


Figure S2. The Charnock parameter C_{ch} obtained by ST4-FAN in boreal winter (a) and summer (b)

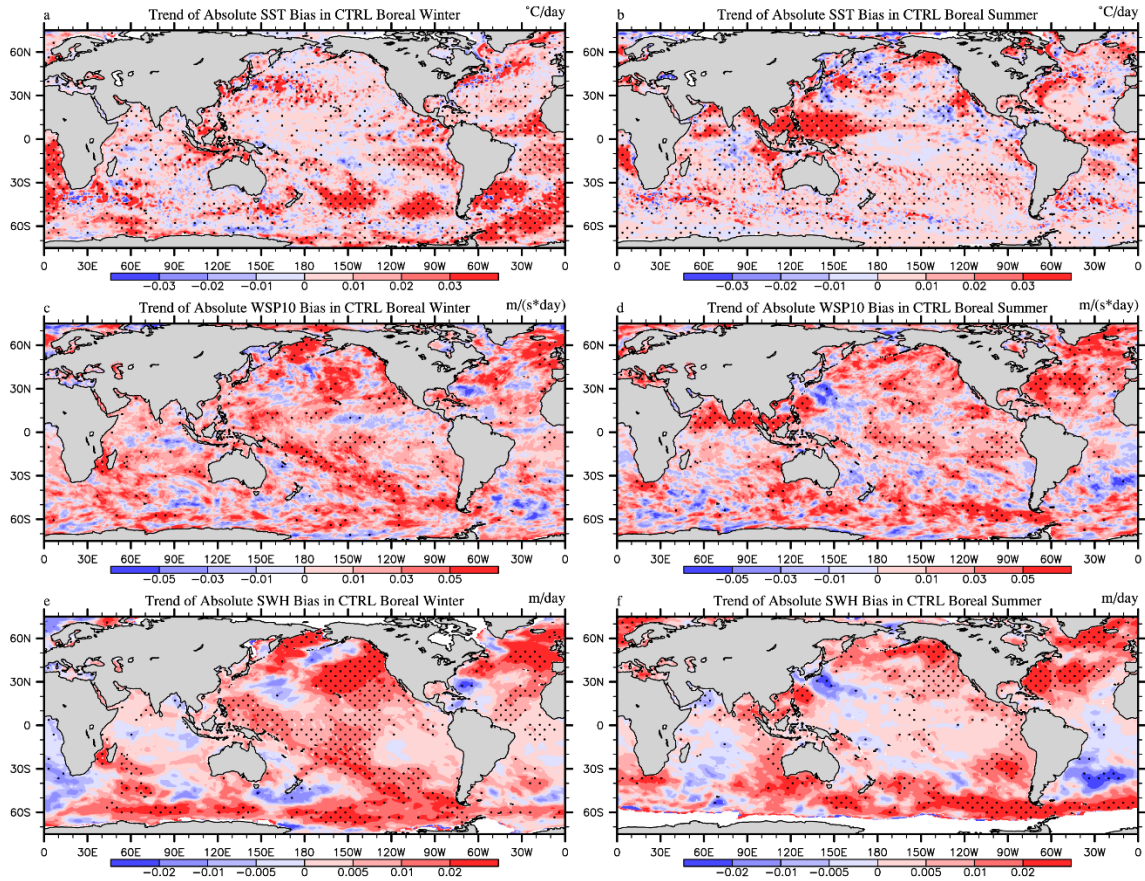


Figure S3. The 53-day regression coefficient (trend) of absolute bias in CTRL; a, b: regression coefficient of absolute SST bias in boreal winter and summer, respectively; c, d: regression coefficient of absolute WSP10 bias in boreal winter and summer, respectively; e, f: regression coefficient of absolute SWH bias in boreal winter and summer, respectively; positive values indicate that the absolute bias (the absolute value of difference between CTRL simulation and OISST/ERA5) increases with time; dotted areas are statistically significant at 95% confidence level.

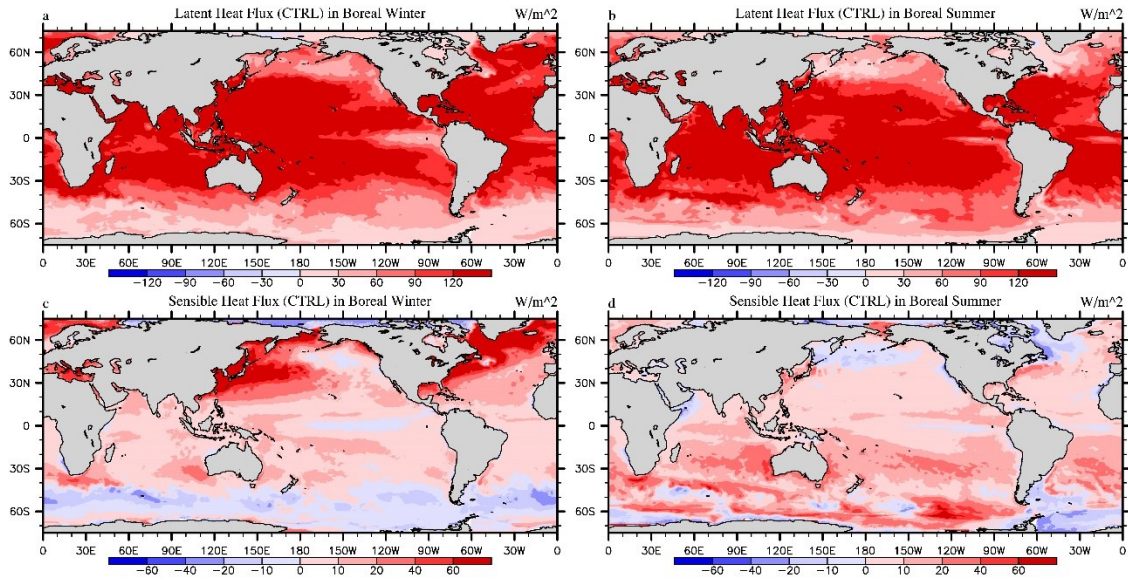


Figure S4. a, b: the 53-day average latent heat flux (W/m^2) in CTRL for Jan-Feb, 2017 and Aug-Sep, 2018; c, d: the average sensible heat flux (W/m^2) in CTRL for Jan-Feb, 2017 and Aug-Sep, 2018; the enthalpy fluxes are positive upwards.

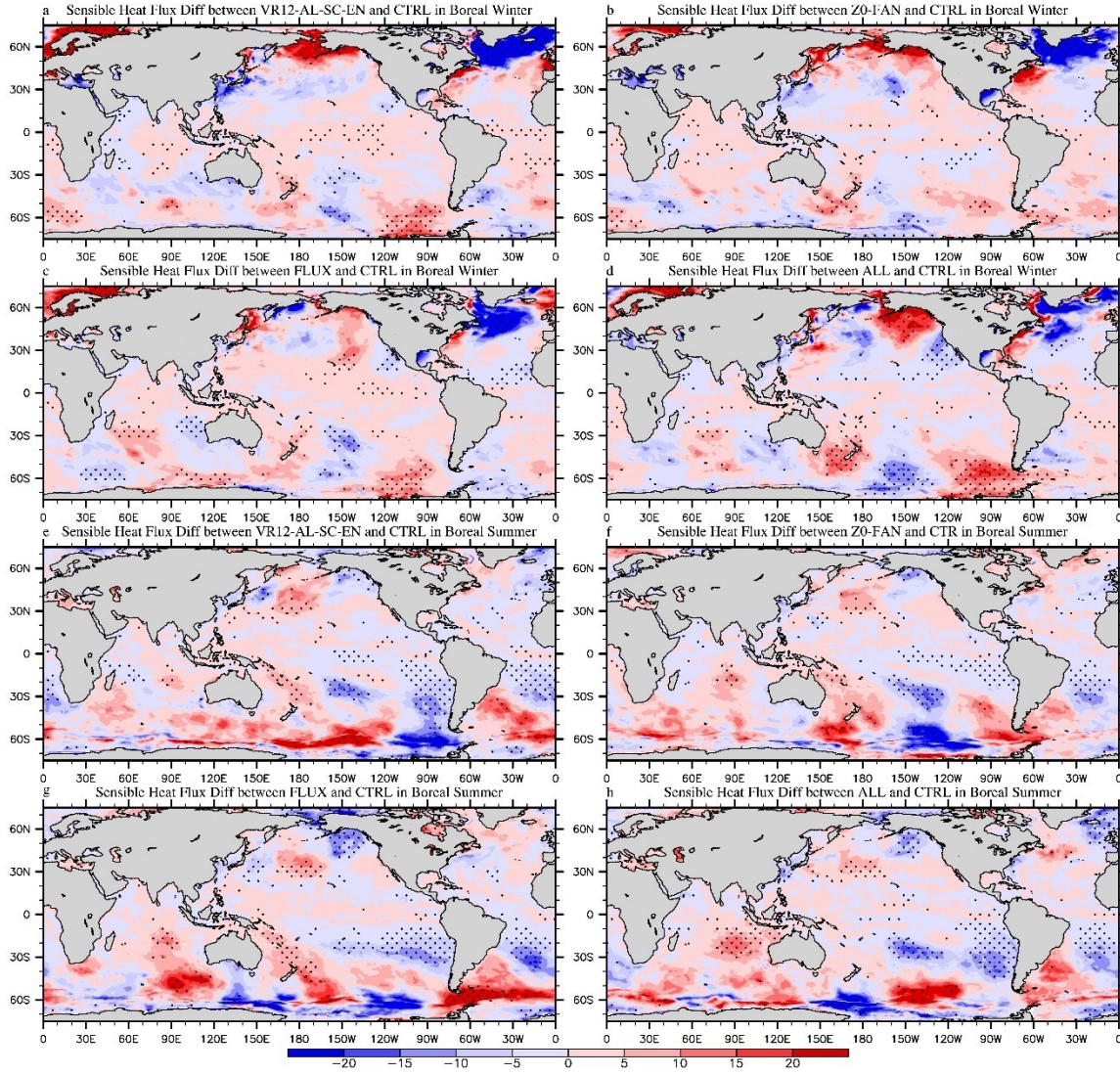


Figure S5. The 53-day average sensible heat flux difference (W/m^2) between 4 sensitivity experiments and CTRL in Jan-Feb, 2017 and Aug-Sep, 2018; a-d: the difference between VR12-AL-SC-EN/Z0-FAN/FLUX/ALL and CTRL (VR12-AL-SC-EN/Z0-FAN/FLUX/ALL minus CTRL) in Jan-Feb, 2017; e-h: the difference between VR12-AL-SC-EN/Z0-FAN/FLUX/ALL and CTRL in Aug-Sep, 2018; the enthalpy fluxes are positive upwards; dotted areas are statistically significant at 95% confidence level.

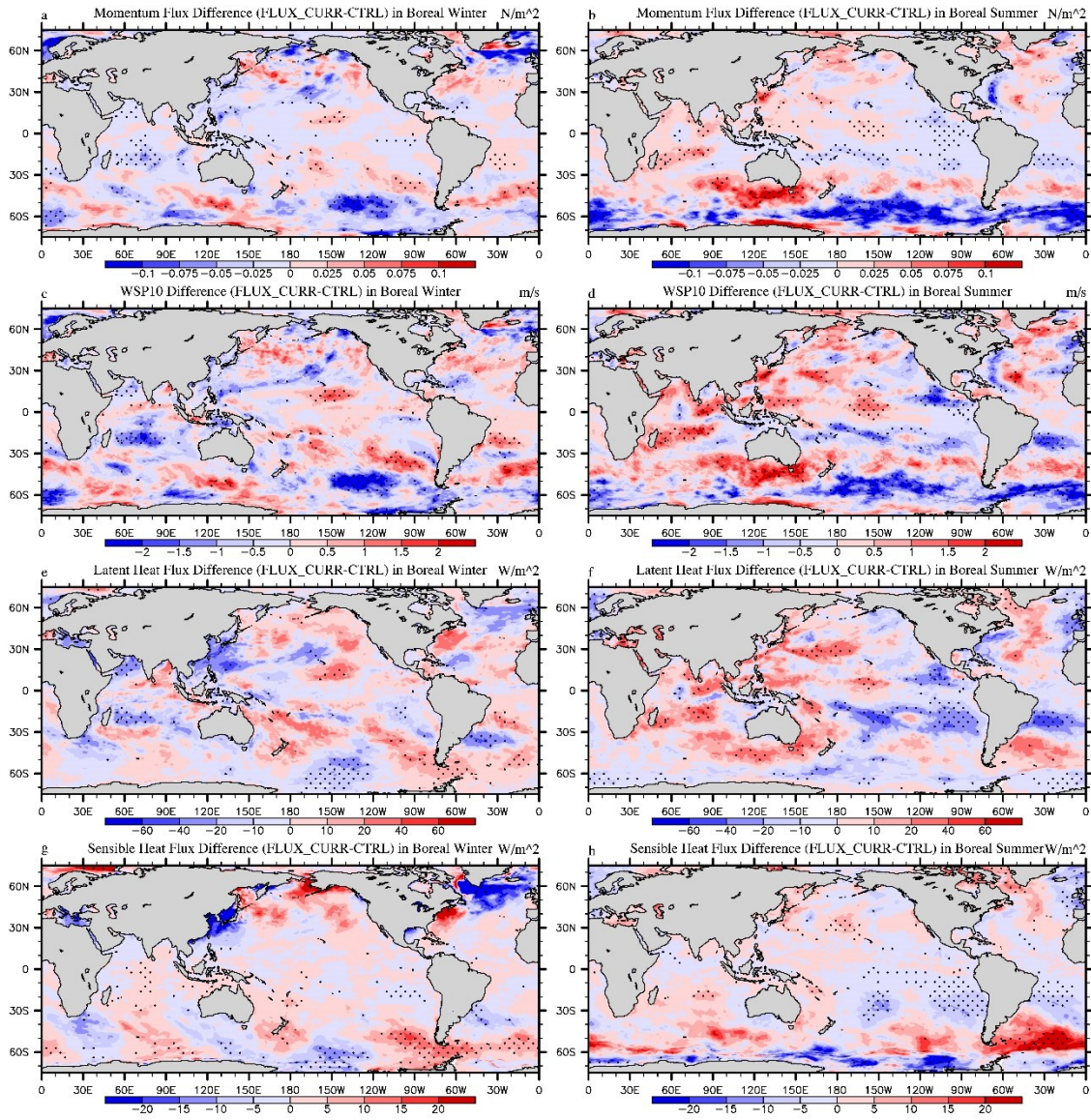


Figure S6. a, b: the 53-day average momentum flux difference between FLUX_CURR and CTRL (FLUX_CURR minus CTRL) in Jan-Feb, 2017 and Aug-Sep, 2018; c, d: the average WSP10 difference between FLUX_CURR and CTRL (FLUX_CURR minus CTRL); e, f: the average latent heat flux difference between FLUX_CURR and CTRL (FLUX_CURR minus CTRL); g, h: the average sensible heat flux difference between FLUX_CURR and CTRL (FLUX_CURR minus CTRL); the enthalpy fluxes are positive upwards; dotted areas are statistically significant at 95% confidence level.

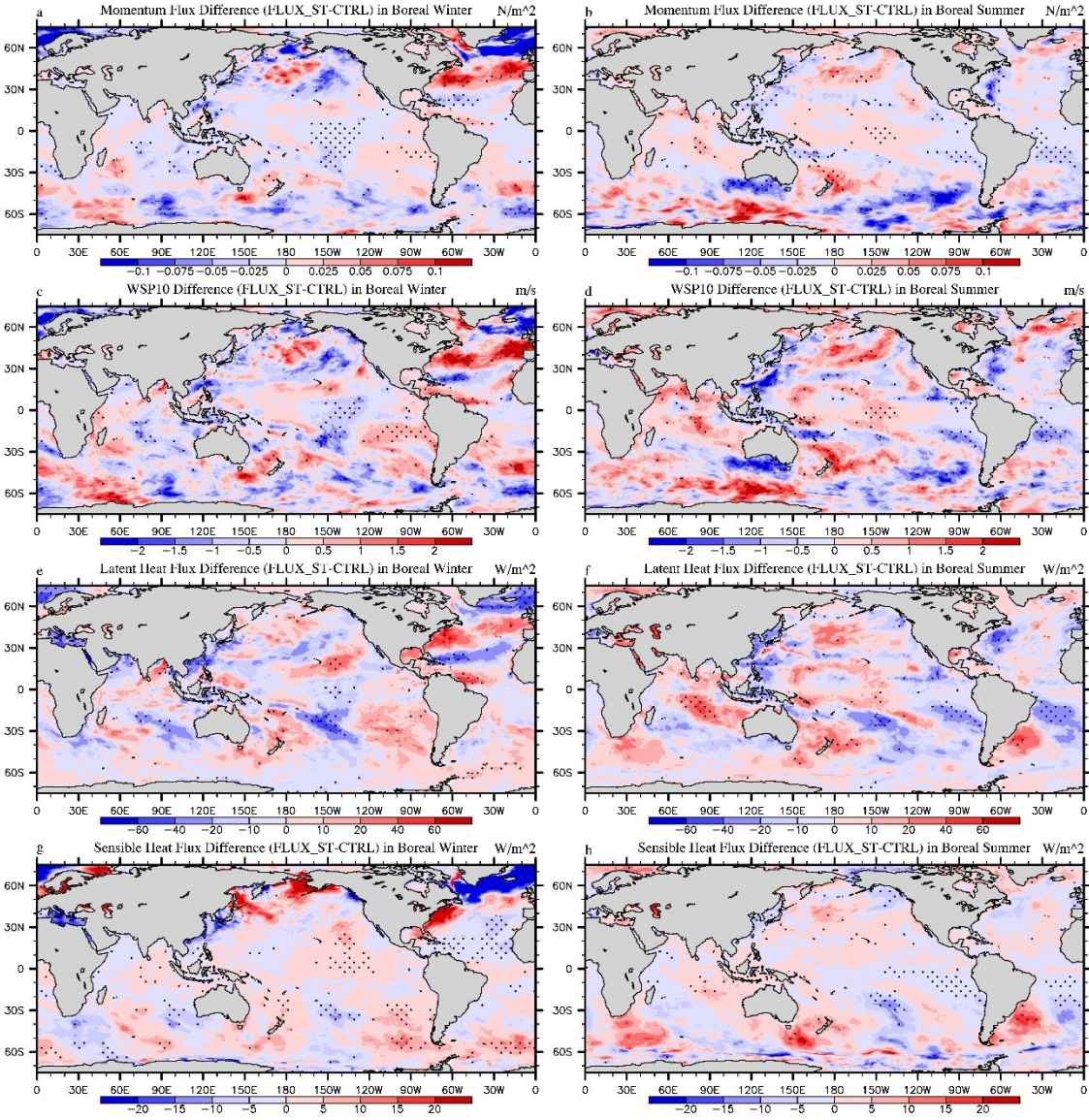


Figure S7. a, b: the 53-day average momentum flux difference between FLUX_ST and CTRL (FLUX_ST minus CTRL) in Jan-Feb, 2017 and Aug-Sep, 2018; c, d: the average WSP10 difference between FLUX_ST and CTRL (FLUX_ST minus CTRL); e, f: the average latent heat flux difference between FLUX_ST and CTRL (FLUX_ST minus CTRL); g, h: the average sensible heat flux difference between FLUX_ST and CTRL (FLUX_ST minus CTRL); the enthalpy fluxes are positive upwards; dotted areas are statistically significant at 95% confidence level.

Table S1. The 28-day global average PRD and daily runtime for SST, SWH and WSP10 in sensitive experiments (the same setups as the ALL experiment in Table 1) with different coupling steps in Jan, 2017; the number of total cores used is 140; in 1_STEP_ALL experiment, three components were coupled every time step; in 5_STEP_ALL (10_STEP_ALL) they were coupled every 5 (10) steps; in 10_STEP_WW3, only the WW3 was coupled every 10 steps, whereas the GFS and the MOM4 maintained the coupling frequency of each step following original settings in CFS.

Experiments	SST PRD	SWH PRD	WSP10 PRD	Daily runtime (s)
1_STEP_ALL	-6.31%	-1.61%	-1.63%	25677
5_STEP_ALL	-6.71%	-0.64%	-0.67%	19546
10_STEP_ALL	-6.56%	-0.37%	-0.83%	19012
10 STEP WW3	-6.11%	-1.43%	-1.63%	19171

Table S2. Correlation coefficient, RMSE and skill score of SWH in WW3 simulations versus Jason-3 observation at 00:00 on Jan 3, 2017; the simulated SWHs were generated by a stand-alone WW3 model (without coupling) with different input-dissipation source terms (ST) and wind forcings (CCMP and ERA5); the RMSE and skill score (SS) are calculated as $\text{RMSE} = \sqrt{\sum_{i=1}^n (\hat{y}_i - y_i)^2 / n}$ and $\text{SS} = 1 - \frac{\sum_{i=1}^n (\hat{y}_i - y_i)^2}{\sum_{i=1}^n ((\hat{y}_i - \bar{y}_i) + |y_i - \bar{y}_i|)^2}$, respectively, where \hat{y}_i is simulated value, y_i is Jason-3 data and \bar{y}_i is the average, $i=1, n$ and $n=2613$ is the total number of measurements in the Jason-3 orbit.

Experiments	Correlation Coefficient (P<0.01)	RMSE	Skill Score
ERA-5 ST2	0.76	0.42	0.85
ERA-5 ST3	0.77	0.41	0.86
ERA-5 ST4	0.82	0.37	0.89
ERA-5 ST6	0.82	0.49	0.86
CCMP ST4	0.69	0.54	0.78
CCMP ST2	0.68	0.59	0.76

Table S3. The 53-day mean absolute percentage error (MAPE) differences for WSP10 between FLUX_CURR/ FLUX_ST/ FLUX and CTRL (MAPE in FLUX_CURR/ FLUX_ST/ FLUX minus MAPE in CTRL); the MAPE is calculated as $\text{MAPE} = \left(\frac{100\%}{n} \right) \sum_{i=1}^n \left| \frac{\hat{y}_i - y_i}{y_i} \right|$, where \hat{y}_i is simulated value, y_i is NDBC buoy observation, $i=1, 53$; UQ, LQ and MD mean the 25% buoys with the highest bias in CTRL, the 25% buoys with the lowest bias in CTRL and the rest 50%; values in brackets are the mean bias in CTRL (CTRL minus NDBC); the asterisk means statistically significant of the difference compared with CTRL at 95% confidence level.

WSP10 MAPE Difference (20170106-20170228) for 374 buoys				
CTRL Bias (m/s)	UQ _{CTRL} (3.28)	LQ _{CTRL} (-1.15)	MD _{CTRL} (0.67)	TOTAL (0.87)
FLUX_CURR	-11.03*	1.69	-0.01	-2.35
FLUX_ST	-6.98*	2.01*	2.61	-0.05
FLUX	-17.31*	-0.05	-1.22*	-4.97*
WSP10 MAPE Difference (20180806-20180928) for 404 buoys				
CTRL Bias (m/s)	(2.43)	(-1.52)	(0.28)	(0.37)
FLUX_CURR	-16.43*	2.78	-0.92*	-3.88*
FLUX_ST	-12.45*	3.12	-0.62*	-2.64*
FLUX	-23.21*	1.25*	-4.04*	-7.51*

Table S4. The NDBC buoy identifiers

201701-02 (WSP)	201701-02 (SWH)	201808-09 (WSP)	201808-09 (SWH)
41002	32012	41002	41002
41004	41002	41004	41004
41008	41004	41008	41008
41013	41008	41009	41009
41024	41025	41010	41010
41025	41040	41013	41013
41029	41041	41024	41025
41033	41043	41025	41040
41037	41044	41029	41041
41038	41046	41033	41043
41040	41047	41037	41044
41041	41048	41038	41046
41043	41049	41041	41047
41044	41052	41043	41048
41046	41053	41044	41049
41047	41056	41046	41052
41048	41060	41047	41053
41049	41108	41048	41056
41052	41110	41049	41060
41053	41112	41052	41110
41056	41113	41053	41112
41064	41114	41056	41113

42001	41115	41062	41114
42002	41116	41063	41115
42003	41159	41064	41117
42012	42001	42001	41118
42013	42002	42002	41159
42019	42003	42003	42001
42020	42012	42012	42002
42022	42019	42013	42003
42023	42020	42019	42012
42035	42035	42020	42019
42036	42036	42022	42020
42039	42039	42023	42035
42043	42040	42039	42039
42044	42055	42040	42040
42045	42056	42043	42055
42047	42058	42055	42056
42055	42059	42056	42057
42056	42067	42057	42060
42058	42085	42060	42079
42059	42097	42085	42085
42067	42098	42360	42097
42085	42099	42395	42098
42088	42360	44007	42099
42090	42369	44009	42360
42360	42375	44013	42395
42361	42392	44014	44005
42362	42395	44017	44007
42364	42887	44018	44008
42369	43010	44025	44009
42375	44005	44027	44013
42395	44007	44029	44014
44005	44011	44030	44017
44007	44013	44032	44018
44013	44014	44033	44025
44014	44017	44034	44027
44024	44024	44037	44029
44027	44025	44039	44030
44029	44027	44040	44032
44030	44029	44042	44033
44032	44030	44058	44034
44033	44032	44063	44037
44034	44033	44064	44039
44037	44034	44065	44040
44039	44037	44066	44042
44040	44042	44069	44056

44042	44056	44072	44058
44058	44058	46001	44062
44062	44062	46002	44063
44065	44065	46005	44064
44069	44066	46011	44065
44072	44072	46012	44066
46001	44089	46013	44072
46006	44090	46014	44086
46011	44091	46025	44087
46012	44093	46026	44089
46013	44097	46027	44090
46014	44098	46029	44091
46015	44099	46035	44095
46022	44100	46042	44097
46025	46001	46050	44098
46026	46002	46053	44099
46027	46006	46054	44100
46028	46011	46059	46001
46029	46012	46060	46002
46035	46013	46069	46005
46041	46014	46072	46011
46047	46015	46073	46012
46050	46022	46075	46013
46053	46025	46076	46014
46054	46026	46077	46025
46059	46027	46078	46026
46060	46028	46080	46027
46061	46029	46081	46028
46066	46035	46082	46029
46069	46041	46083	46035
46070	46042	46084	46042
46073	46047	46085	46047
46076	46050	46086	46050
46080	46054	46087	46053
46081	46059	46088	46054
46083	46060	46089	46059
46085	46061	46092	46060
46086	46066	46096	46066
46087	46069	46097	46069
46088	46070	46098	46072
46092	46071	46099	46073
46097	46073	46100	46075
46098	46075	46125	46076
46100	46076	46128	46077
46120	46078	51000	46078

51000	46080	51001	46080
51001	46081	51002	46081
51002	46083	51003	46082
51003	46084	51004	46083
51004	46085	51101	46084
51101	46086	aamc1	46085
aamc1	46087	adka2	46086
adka2	46088	agxc1	46087
agxc1	46108	alia2	46088
amaa2	46114	amaa2	46089
amrl1	46211	amrl1	46108
anta2	46213	anpt2	46114
apr7	46214	anta2	46211
asto3	46215	anvc1	46213
atka2	46217	apcf1	46214
awrt2	46218	apr7	46215
babt2	46219	arop4	46217
bara9	46221	asto3	46218
baxc1	46222	atka2	46219
bepb6	46224	auga2	46221
bism2	46225	awrt2	46222
blia2	46229	babt2	46224
blta2	46232	baxc1	46225
bltm2	46237	bepb6	46229
brhc3	46239	bftn7	46232
bsca1	46240	bgcf1	46235
burl1	46242	bism2	46237
buzm3	46243	blta2	46239
camm2	46244	brhc3	46240
cap11	46246	brnd1	46242
cbbv2	46248	bsca1	46243
cdea2	46251	burl1	46244
cdrf1	46253	buzm3	46246
cecc1	46254	bzst2	46248
cfwm1	46255	cap11	46251
chao3	46256	cdrf1	46253
chsv3	46257	cdxa2	46254
chts1	46258	cecc1	46256
clbf1	46259	chao3	46258
clk7	51000	chbv2	46259
cman4	51001	chsv3	46262
covm2	51002	chts1	46263
cpmw1	51003	chqv2	46264
cpnt2	51004	clbf1	46265
crtal1	51101	clk7	51000

cryv2	51201	cman4	51001
cspa2	51202	covm2	51002
cwbfl	51203	cpmw1	51003
deld1	51204	cpxc1	51004
dkcm6	51205	crtal1	51101
dpii1	51206	cryv2	51202
dukn7	51207	cspa2	51205
einl1	51208	cwbfl	51206
eptt2	51210	domv2	51207
espp4	52200	dpii1	51208
fbis1	52201	drfa2	51209
fegt2	52202	dukn7	51210
ffia2	bthd1	einl1	51211
fhpf1	grbl1	emat2	51212
fila2	ljpc1	eptt2	51213
fmoa1	lopl1	erxa2	52200
fmrf1	ocsm2	espp4	52201
fpkg1	ssbn7	fbis1	52202
frdf1		fegt2	52211
frdp4		fhpf1	frfn7
frwl1		fila2	ljpc1
fskm2		fmoa1	lopl1
fsnm2		fmrf1	ocsm2
fwyf1		fpkg1	ssbn7
gis11		fpst2	
gnjt2		fskm2	
grrt2		fsnm2	
hbyc1		ftpc1	
hist2		fwyf1	
hmsa2		gis11	
icac1		gnjt2	
iiwc1		grrt2	
iloh1		gtot2	
imgp4		guxa2	
iosn3		hbyc1	
irdt2		hcg7	
jmpn7		hist2	
kata1		hmsa2	
keca2		icac1	
kgca2		icya2	
klih1		iloh1	
kptv2		iosn3	
kwhh1		irdt2	
kywf1		jmpn7	
lapw1		kata1	

lcna2	kdaa2
lkwf1	keca2
lndc1	kexa2
lonf1	kgca2
lop11	klih1
luit2	kptv2
lwsd1	ktnf1
lwtv2	kwhh1
mbet2	kywf1
mbla1	lapw1
mcga1	lixa2
mgip4	ljac1
mgzp4	ljpc1
mism1	lkwf1
mlrf1	lndc1
mnpv2	lop11
mokh1	luit2
mqtt2	lwsd1
mrya2	mbet2
mtbf1	mbla1
mypf1	meyc1
ncdv2	mgip4
nkta2	mism1
nstp6	mnpv2
ntbc1	mokh1
ntkm3	mqtt2
nwhc3	mrna2
nypo3	mrya2
nwpr1	mypf1
nwwh1	nkla2
okxc1	nkta2
olsa2	nkxa2
omhc1	nmta2
ouuh1	npsf1
optf1	nstp6
pacf1	ntbc1
pact2	ntkm3
pcbf1	nwhc3
pcgt2	nypo3
pclf1	nwpr1
pcnt2	nwwh1
pfdc1	ocim2
pfxc1	okxc1
pgbp7	olsa2
pila2	omhc1

pill1	oouh1
plsf1	optf1
plxa2	orin7
poro3	pact2
port2	paxa2
ppta1	pcbf1
pptm2	pcgt2
ppxc1	pcnt2
prda2	pegf1
prjc1	pfdc1
prta2	pfxc1
psbm1	pgbp7
pstl1	pgxa2
psxc1	pila2
ptat2	poro3
ptaw1	port2
ptbm6	pptm2
ptgc1	ppxc1
ptit2	prda2
ptla2	prjc1
ptrp4	pryc1
ptww1	psbm1
pvgf1	pslc1
pxac1	pstl1
pxoc1	psxc1
qptr1	ptat2
rarm6	ptaw1
rcmc1	ptbm6
rept2	ptcr1
rlit2	ptgc1
rlot2	ptit2
rplv2	ptla2
rsjt2	ptrp4
rtat2	ptww1
rtyc1	pvgf1
sanf1	pxac1
sapf1	pxoc1
sauf1	qptr1
sbeo3	rcmc1
sbpt2	rdda2
sgnt2	rixa2
sgof1	rlit2
shbl1	rplv2
shpf1	rsjt2
sipf1	rtat2

sjnp4	rtyc1
sjsn4	sapf1
slim2	saufl
spgf1	sbeo3
srst2	sbpt2
tcbm2	sgnt2
tokw1	shbl1
tpaf1	shpf1
tplm2	shxa2
trdf1	sipf1
tshf1	sisw1
txpt2	sjnp4
ulra2	sjsn4
unla2	slim2
vakf1	smkf1
vcaf1	spgf1
vcat2	srst2
vcva2	stxa2
vqsp4	tcbm2
wakp8	tokw1
wdel1	tpaf1
welm1	tplm2
wptw1	trdf1
wycm6	txpt2
yabp4	unla2
DM186A	vcaf1
DM172A	vcat2
DM227A	vcva2
DM221A	venf1
DM214A	wahv2
DM193A	wakp8
DM207A	wptw1
M179A-	wycm6
DM138A	ykrv2
DM228A	yktv2
DM165A	DM281A
DM220A	DM221A
DM192A	DM316A
DM206A	DM309A
DM201A	DM247B
M178A-	DM260A
DM185A	DM302A
DM171A	DM295A
DM226A	M274A-
DM167A	DM282A

DM222A	DM220A
DM213A	DM315A
DM194A	DM268A
DM208A	DM310A
DM199A	DM289A
DM139A	DM261A
DM229A	DM301A
DM164A	DM252A
DM219A	DM296A
DM216A	M273A-
DM191A	DM280A
DM205A	DM226A
DM202A	DM222A
DM184A	DM317A
DM170A	DM266A
DM225A	DM308A
DM168A	DM287A
DM223A	DM259A
DM212A	DM303A
DM195A	DM294A
DM209A	M275A-
DM198A	DM283A
DM140A	DM229A
DM175A	DM219A
DM230A	DM314A
DM190A	DM269A
DM204A	DM311A
DM203A	DM191A
DM183A	DM290A
DM169A	DM262A
DM224A	DM300A
DM211A	DM297A
DM196A	M272A-
DM210A	DM279A
DM197A	DM225A
DM163A	DM223A
DM218A	DM318A
	DM265A
	DM307A
	DM286A
	DM258A
	DM304A
	DM293A
	M276A-
	DM284A

DM230A
DM270A
DM312A
DM245A
DM245B
DM263A
DM299A
DM250A
DM298A
M271A-
DM278A
DM224A
DM319A
DM264A
DM306A
DM196A
DM257A
DM305A
DM292A
M277A-
DM218A
DM313A
